

# **Report on Recent Upgrades to the Curved Duct Test Rig at NASA Langley Research Center**

by

Carl H. Gerhold<sup>1</sup>

Martha C. Brown<sup>2</sup>

Michael G. Jones<sup>3</sup>

Brian M. Howerton<sup>4</sup>

NASA Langley Research Center

Hampton, Virginia

## **ABSTRACT**

**The Curved Duct Test Rig (CDTR) is an experimental facility that is designed to assess the acoustic and aerodynamic performance of aircraft engine nacelle liners in close to full scale. The test section is between 25% and 100% of the scale of aft bypass ducts of aircraft engines ranging in size from business jet to large commercial passenger jet. The CDTR has been relocated and now shares space with the Grazing Flow Impedance Tube in the Liner Technology Facility at NASA Langley Research Center. As a result of the relocation, research air is supplied to the CDTR from a 50,000 cfm centrifugal fan. This new air supply enables testing of acoustic liner samples at up to Mach 0.500. This paper documents experiments and analysis on a baseline liner sample, which the authors had analyzed and reported on prior to the move to the new facility. In the present paper, the experimental results are compared to those obtained previously in order to ensure continuity of the experimental capability. Experiments that take advantage of the facility's expanded capabilities are also reported. Data analysis features that enhance understanding of the physical properties of liner performance are introduced. The liner attenuation is shown to depend on the mode that is incident on the liner test section. The relevant parameter is the mode cut-on ratio, which determines the angle at which the sound wave is incident on the liner surface. The scattering of energy from the incident mode into higher order, less attenuated modes is demonstrated. The configuration of the acoustic treatment, in this case lined on one surface and hard wall on the opposite surface, is shown to affect the mode energy redistribution.**

---

<sup>1</sup> Senior Research Scientist, Research Directorate, Aeroacoustics Branch, Associate Fellow, AIAA, phone: (757) 864-5279, email: [carl.h.gerhold@nasa.gov](mailto:carl.h.gerhold@nasa.gov)

<sup>2</sup> Aerospace Engineer, Research Directorate, Aeroacoustics Branch, phone: (757) 864-6277, email: [martha.c.brown@nasa.gov](mailto:martha.c.brown@nasa.gov)

<sup>3</sup> Senior Research Scientist, Research Directorate, Structural Acoustics Branch, Associate Fellow, AIAA, phone: (757) 864-5272, email: [michael.g.jones@nasa.gov](mailto:michael.g.jones@nasa.gov)

<sup>4</sup> Aerospace Engineer, Research Directorate, Structural Acoustics Branch, Senior Member, AIAA, phone: (757) 864-8365, email: [brian.m.howerton@nasa.gov](mailto:brian.m.howerton@nasa.gov)

## Nomenclature

$\rho_o, c_o$	= density and sound speed in air, $\text{kg/m}^3$ , $\text{m/s}$
$i$	= $\sqrt{-1}$ , unit imaginary number
$p$	= acoustic pressure, Pa
$M$	= uniform mean flow Mach number
$k$	= $\omega/c_o$ , freespace wavenumber, $\text{m}^{-1}$
$k_{xy}$	= transverse wavenumber, $\text{m}^{-1}$
$k_z$	= axial wavenumber, $\text{m}^{-1}$
$a$	= horizontal duct dimension, m
$b$	= vertical duct dimension, m
$n$	= horizontal mode order
$m$	= vertical mode order
$\omega$	= angular frequency, $\text{s}^{-1}$
$\alpha$	= absorption coefficient
$\theta$	= acoustic liner resistance, normalized by $\rho_o c_o$
$\chi$	= acoustic liner reactance, normalized by $\rho_o c_o$
$\phi$	= angle of incidence

## I. Introduction

Despite significant strides in aircraft power plant design for noise control, notably the high bypass ratio engine, the aircraft engine remains a major source of overall aircraft noise. The high bypass ratio engine configuration uses the low-pressure turbine to drive a large diameter fan, and it is the fan that provides most of the engine thrust. The fan is the major noise source with a noise signature characterized by tones at the blade passage frequency as well as broadband noise [1]. Fan noise reductions have been achieved by the installation of passive acoustic liners in both the nacelle inlet and aft ducts to attenuate tonal and broadband components. The nacelle adds weight and drag, which increases specific fuel consumption, and thus the designer must reconcile two conflicting criteria: maximizing liner treatment for noise control and minimizing nacelle size. It is critical to develop a liner design that provides a targeted noise reduction spectrum by making the most effective use of available treatment area. This, in turn, requires greater knowledge of how noise propagates through the duct than is currently available. One purpose of the Curved Duct Test Rig (CDTR) is to provide a test-bed for generation and propagation of realistic sounds

in a large-scale duct, representative of the aft bypass duct, and for evaluation of noise control methodologies.

The CDTR is designed to evaluate innovative duct noise control technologies as well as standard liner designs that are currently in use in engines. The liner samples are of a scale that is representative of those that can be found in existing engines. While the actual engine environment can't be replicated in the laboratory, certain aspects, namely, representative Mach number flow and higher order mode incident sound, are capabilities unique to the CDTR. Some of the liner samples are industry-designed and fabricated, allowing the effect of manufacturing methods to be investigated. A liner sample was fabricated and tested to provide a baseline for the data analysis process. This liner was designed to provide the maximum attenuation in the middle of the useable frequency range ( $\sim 1500$  Hz) and at the maximum flow speed (Mach 0.275) of the CDTR at the time. The authors reported on evaluations of this in-house-designed liner (Liner L01) in a previous paper [2].

As part of the laboratory consolidation effort at NASA Langley Research Center, the Curved Duct Test Rig (CDTR) was moved to a laboratory space designated the Liner Technology Facility (LTF). The CDTR occupies the space together with the Grazing Flow Impedance Tube, which is described in [3]. The combined laboratory has the tools to perform research on acoustic liners ranging from fundamental descriptions of the impedance parameters to investigation of the effects of duct curvature and the presence of higher order modes on liner performance. A significant upgrade to the CDTR that resulted from the relocation is the installation of a 52,000 cfm centrifugal fan. This fan enables tests to be performed on liner samples at speeds in the test section of up to Mach 0.500.

When the upgraded laboratory was opened, the authors retested liner L01. One purpose of this series of tests is to verify that conditions in the new facility are comparable to those in the previous configuration and that the results are repeatable. This paper discusses the repeatability of the results. Another aim of the tests is to evaluate liner performance utilizing the upgraded test conditions provided by the laboratory. This paper discusses the performance of the in-house liner at Mach 0.500. The authors are constantly evolving data analysis methods in the effort to learn more about the physics of liner behavior. In this paper, results are analyzed with an aim toward gaining more insight into the effect of liner configuration on acoustic performance.

## **II. Description of the facility**

The CDTR is an open circuit wind tunnel that uses a fan to draw unconditioned atmospheric air through the test section, as shown in Figure 1. All equipment upstream of transition 1 and downstream of transition 2 constitutes the new configuration. The flow delivery system consists

of an inlet housing to prevent debris/water ingestion, an air inlet that is contoured to minimize distortion, 60 inch x 30 inch vertical duct, a 90° bend of 3.75 foot average radius, and a 60 inch x 30 inch to 30 inch x 30 inch transition (transition 1). The bend contains turning vanes to improve the uniformity of flow. Downstream of the transition is the test section of the original CDTR, which was transferred from the previous location in the Anechoic Noise Research Laboratory. This duct consists of a flow conditioning section with screens and honeycomb, transition to 6 inch x 15 inch test section dimension, loudspeaker section, upstream microphone section, liner test section box, downstream microphone section, and diffuser/anechoic termination. Downstream of the test section is a transition to a 39 inch x 39 inch duct (transition 2), resonator, muffler, and the fan. The fan is a centrifugal fan rated at 52,000 cfm and driven by a 600 HP motor. The muffler reduces fan noise in the test section in the audible frequencies, above 500 Hz. The resonator was designed to reduce the low frequency fan noise in the range from 63 to 500 Hz. While the sound in range of frequencies between 63 and 250 Hz is not used to assess liner attenuation, the fan noise driving the microphones at these low frequencies reduces their effective dynamic range. Thus the microphone sensitivity is improved by reducing the fan noise in the 63-500 Hz frequencies using the resonator. The muffler and resonator are designed to reduce the fan-generated noise to 10 dB below the expected flow noise in the test section at Mach 0.50.

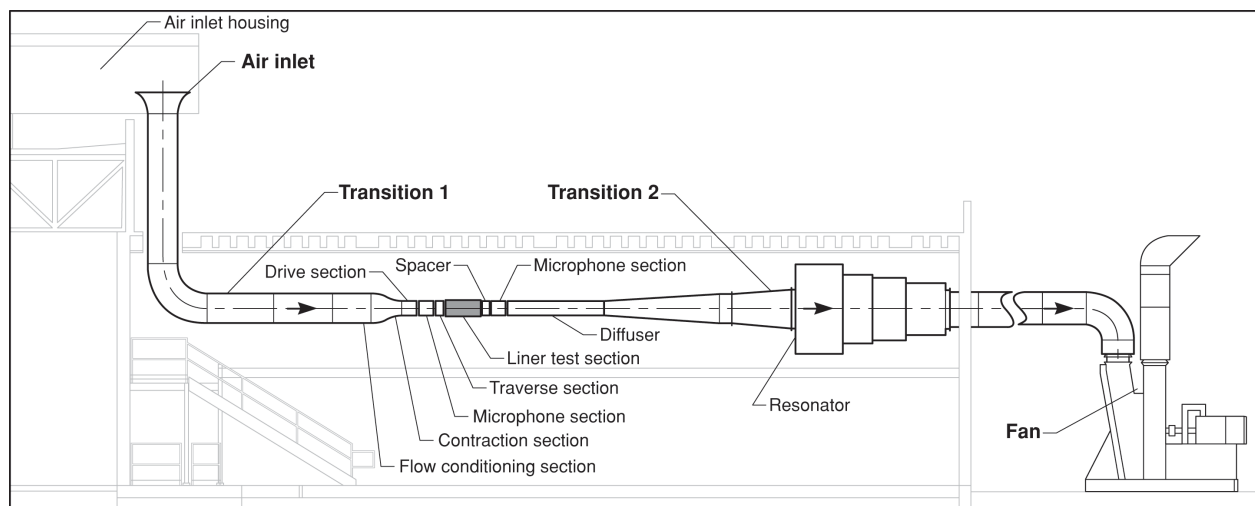


Figure 1. Drawing of the Curved Duct Test Rig layout in the Liner Technology Facility.

Sound in the duct is generated by an array of 16 loudspeakers. The magnitude and phase of the voltage signal to each loudspeaker is controlled such that a selected mode can be generated in the duct. A subset of the upstream microphone array is used as the control to adjust the signals to the loudspeakers. The microphone and loudspeaker arrays and the sound control system are described in a previous paper [4]. The recorded signals from the upstream and downstream

microphone arrays are analyzed to determine the mode distribution of sound in the duct incident upon and discharged from the liner test section, as discussed in previous papers [4,5]. The analysis at each frequency includes all the modes that are cut on at that frequency as well as the two cut-off modes that are closest to cut-on.

Figure 2 shows a typical modal power distribution upstream of the liner test section at Mach 0.275. In this case, the (0,0) mode is generated in the duct, where modes are ordered as (vertical, horizontal). The other modes in the duct, in addition to the generated mode, are plotted, and the frequencies at which they cut on are listed in the key. The routine to determine the mode amplitudes at a particular frequency includes the cut-on modes and the first two cut-off modes at that frequency. The target sound level of the generated tone is 130 dB. It is seen in Figure 2 that the (0,0) mode component equals the target level of 130 dB to within  $\pm 1$  dB at frequencies up to 1900 Hz. The (0,0) mode is dominant to 2300 Hz and is at least 10 dB greater than the next mode up to 2100 Hz. The design goal for the sound control system was for the target mode sound power to be at least 10 dB greater than any other mode component. The design goal is met for the (0,0) mode at Mach 0.275 up to 2100 Hz, above which frequency the number of modes to be suppressed overtaxes the control authority. It is generally found that the design goal is met out to higher frequencies as higher order modes are specified. Given that the sound power distribution upstream of the liner is dominated by the target mode, the downstream modal distribution can be assessed relative to an upstream sound consisting of the target mode only.

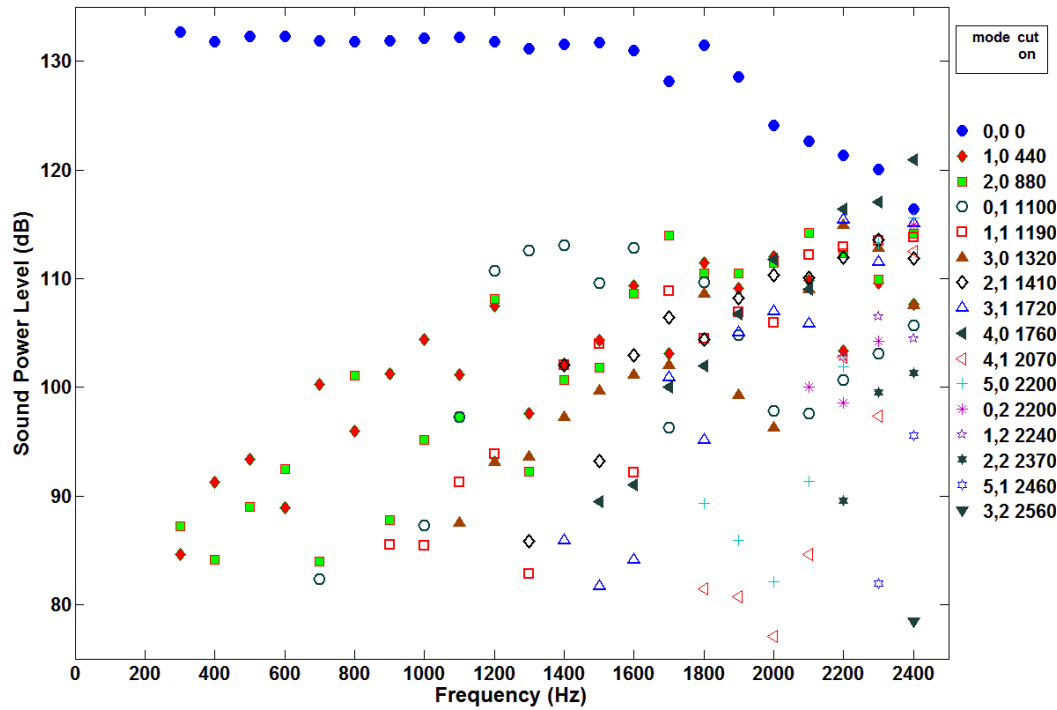


Figure 2. Mode distribution upstream of liner test section, (0,0) mode generated in the duct, flow speed Mach 0.275. Data acquired in 2010.

### III. Results

The test set up is shown in Figure 3. It consists of the in-house-designed liner (identified as liner L01) on the left side of the duct as shown in Figure 3 and a hard wall on the right side. This experiment set up is baseline configuration and it is given the designation L01R. The L01 liner is a single degree-of-freedom perforate-over-honeycomb liner with a core depth of 1.50 inch. The perforate is 0.040 inch thick and is 8.9% open with 0.039 inch diameter holes. The hard wall is fabricated from solid sheet over honeycomb core. The honeycomb core is 0.75 inch thick and the cover sheet is 0.040 inch thick. This liner configuration was tested in 2006, before the upgrades to the facility were performed [2].

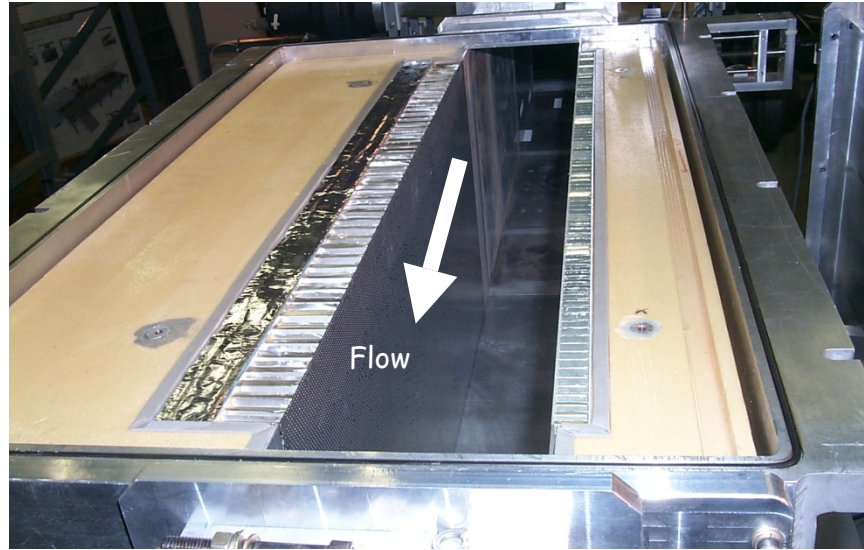


Figure 3. Liner configuration L01R with 1.5 inch thick liner on the left side as shown. The liner on the right wall has a solid cover sheet to achieve hard wall. View looking upstream.

### A. Repeatability

A series of tests was run to determine whether the change in air delivery, from pushing by a high-pressure source to pulling by a fan, affects the acoustic performance of the CDTR. Figure 4 shows the overall attenuation by the liner, comparing measured results from data acquired in the previous set-up, designated 2006, to those acquired in the present configuration, designated 2010. The (0,0) mode is generated in the duct and the flow speed is Mach 0.275. The two curves are quite similar and agree to within 1.0 dB. Both show peak attenuation of approximately 20 dB at a frequency between 1200 and 1300Hz. The curves indicate that the peak attenuation occurs at slightly different frequencies within the 1200-1300 Hz band. The likely cause of this shift in the frequency of the peak is the different temperatures of the air in the duct due to the fact that the experiments were performed at different times of the year. The difference between the two curves above 2000 Hz is likely due to the fact that the (0,0) mode is not dominant in the duct above 2000 Hz, as was seen in Figure 2. An uncertainty analysis is planned to categorize and quantify the conditions that affect the acoustic performance. Similar comparisons, not shown here, were made with higher-order modes incident on the liner test section at Mach 0.275 and Mach 0.000. The favorable comparison between data acquired in the Curved Duct Rig in the two configurations indicates that change in air delivery does not significantly compromise the experimental rig.

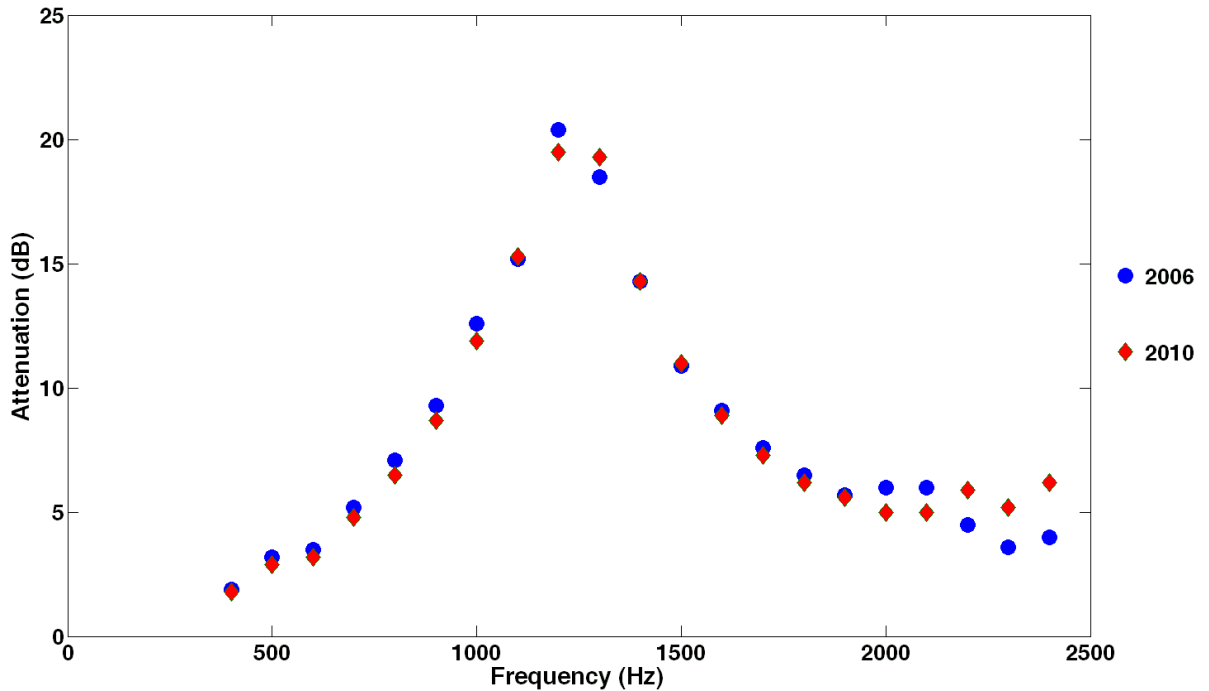


Figure 4. Overall attenuation by liner L01R, (0,0) mode incident, flow speed Mach 0.275. Compares acoustic results obtained before and after facility upgrade.

## B. Effect of flow speed on liner acoustic performance

The maximum test section flow speed that was achievable in the previous set-up was Mach 0.275. The new fan set-up permits evaluation of liners at grazing flow speeds up to Mach 0.500. This speed is more representative of the flow speeds encountered in an engine aft bypass duct. The overall attenuation with the (0,0) incident on liner L01R at flow speed Mach 0.500 is shown in Figure 5. Also shown in the plot are the attenuation at Mach 0.000 and Mach 0.275. The peak in the attenuation curve shifts toward higher frequencies with increasing flow speed, from 1000 Hz at Mach 0.000, to 1250 Hz at Mach 0.275, to above 1500 Hz at Mach 0.500. The attenuation curve broadens significantly at Mach 0.500. The magnitude of the peak attenuation is considerably greater at Mach 0.275 than it is at Mach 0.000 or at Mach 0.500, indicating that Mach 0.275 is the flow rate near which the optimum liner impedance is achieved in the frequency range.

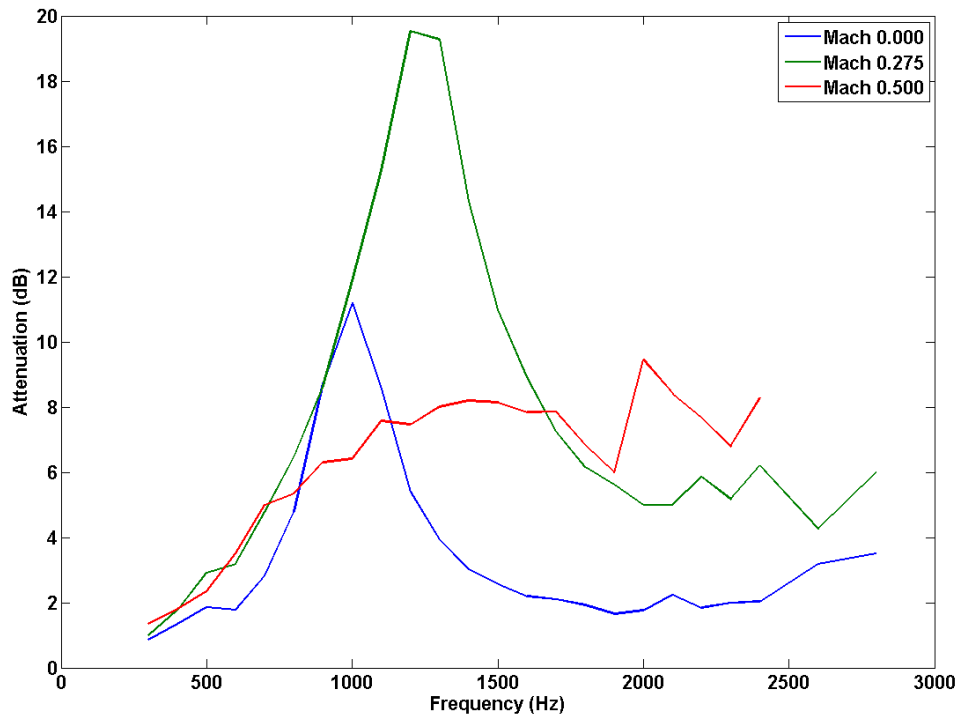


Figure 5. Overall attenuation of (0,0) mode by liner L01R, compares effect of flow speed in the CDTR. Data acquired in 2010.

#### 1. Data Processing: Results at Mach 0.275

Analysis of the data from microphone arrays upstream and downstream of the liner test section includes decomposition of the sound power into the duct modes [2,5]. Mode numbers are identified as (Vertical, Horizontal), where the vertical dimension is 15 inches and the horizontal dimension is 6 inches. Liner acoustic performance is evaluated by determining the modal structure of the sound exiting the liner test section in comparison to the modal structure of the sound that is incident on the liner test section. Additionally, summing the acoustic energy in the hard wall duct downstream of the liner test section and subtracting it from the total energy incident upon the liner test section determine the overall sound reduction for a specific mode input.

The overall attenuation at Mach 0.275 with various modes generated upstream of the liner test section is plotted in Figure 6. The figure shows a composite of the separate experiments in which the indicated mode was generated. Two features are of interest in the plot. The first involves the three lower modes (0,0), (1,0), (2,0), which cut on well below first resonance of the liner (~1250 Hz). The magnitude of the attenuation at the peak increases as the vertical mode order increases, or in order of increasing cut-on frequency. At frequencies beyond the resonance, the attenuation falls off for these modes, as would be expected, since the impedance is heading toward the first

anti-resonance. The other feature involves the higher order modes that cut on near or above the resonance frequency. The attenuation of these modes is higher above 1500 Hz than that shown for the lower orders. Motsinger and Kraft [6] show that the absorption,  $\alpha$ , of sound by the liner depends not only on the normalized impedance,  $\theta + i\chi$ , but also on the angle of incidence:

$$\alpha = \frac{4\theta \cos \varphi}{(1 + \theta \cos \varphi)^2 + (\chi \cos \varphi)^2} \quad (1)$$

For any value of impedance the absorption is maximum when the wave is incident normal to the surface and it decreases toward 0 as the incidence angle approaches 90° (grazing flow).

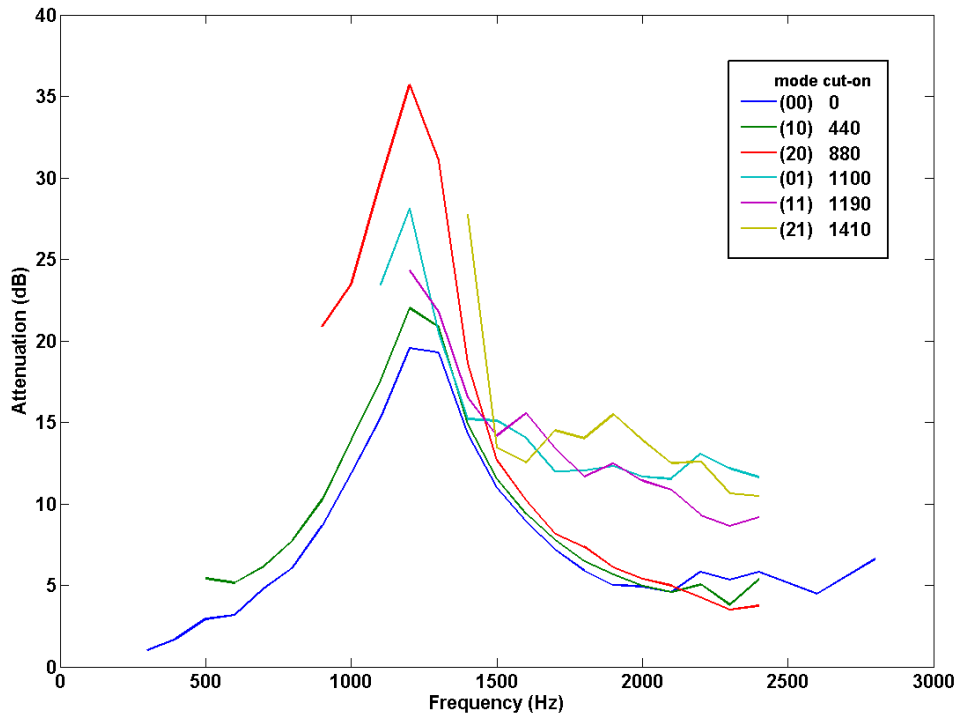


Figure 6. Attenuation of specified mode incident on liner test section with liner L01R at Mach 0.275

Rice and Heidman [7] show that the angle with which the sound wave impinges on the side wall of the duct is a function of the wavenumber:

$$\sin \varphi = \frac{k_z}{k(1 - M \frac{k_z}{k})} \quad (2)$$

where:

$$k_z = \frac{k}{(1-M^2)} \left[ -M + \sqrt{1 - (1-M^2) \left( \frac{k_{xy}}{k} \right)^2} \right] \quad (3)$$

$k_z$  is the axial wavenumber and  $k_{xy}$  is the transverse wavenumber. In the hard wall duct, horizontal dimension  $a$  and vertical dimension  $b$ , the transverse wavenumber is defined by:

$$k_{xy} = \sqrt{\left( \frac{n\pi}{a} \right)^2 + \left( \frac{m\pi}{b} \right)^2}$$

At frequencies below which the term under the radical in equation 3 is negative,  $k_z$  is imaginary and the wave decays exponentially in the axial direction. The wave will propagate at frequencies above which the term in the brackets in equation 3 is real and positive. The frequency at which the term under the radical equals zero is generally considered the mode cut-on frequency. The wavenumber at cut-on is:

$$k_{co} = k_{xy} \sqrt{1 - M^2} \quad (4)$$

At cut-on, the axial wavenumber,  $k_z$  approaches 0 and the incidence angle, from equation 2, is nearly  $0^\circ$ , indicating that the wave front is impinging normal on the duct side wall. At frequencies well above the cut-on,  $k_z$  approaches  $k$ , or  $\phi$  approaches  $90^\circ$ . In this case, the wave front moves tangential to the lined duct wall.

From equation 1 the closer the wavefront impingement on the liner is to normal, the more efficient the liner is at absorbing sound. And from equation 2, the closer the wave is to cut-on, the more normal the wavefront impingement. Thus, from Figure 5, the (2,0) mode, which is closer to cut on at 1250 Hz, is attenuated more than the (1,0) mode, and in turn the (1,0) mode is attenuated more than the (0,0). Likewise, at frequencies above 1250 Hz, higher-order modes are just cutting on while the lower order modes are well cut-on. Thus the higher-order mode wavefronts are directed normal to the liner while the lower-order modes are directed down the duct, and the absorption of the higher-order modes is greater than it is for the lower-order modes.

A notable exception to this trend is the (0,1) mode, which is closest to cut-on at 1250 Hz but is not the most attenuated. This will be discussed further in the next section.

Mode distribution analysis:

The modal distribution of sound power upstream of the liner when the (0,0) mode is generated was shown previously in Figure 2. That figure showed that the target mode, (0,0) was dominant in the duct upstream of the liner at least up to 2300 Hz. The modal distribution of sound power downstream of the liner test section for the (0,0) mode generated at Mach 0.275 is shown in Figure 7. The (0,0) mode dominates through the spectrum below 1300 Hz, where the attenuation of the (0,0) mode is maximum. Energy is scattered into the (0,1) mode and the overall sound downstream of the liner, while mostly comprised of the (0,0) mode, is weakly influenced by the (0,1) mode in the frequencies at and above the frequency of peak attenuation.

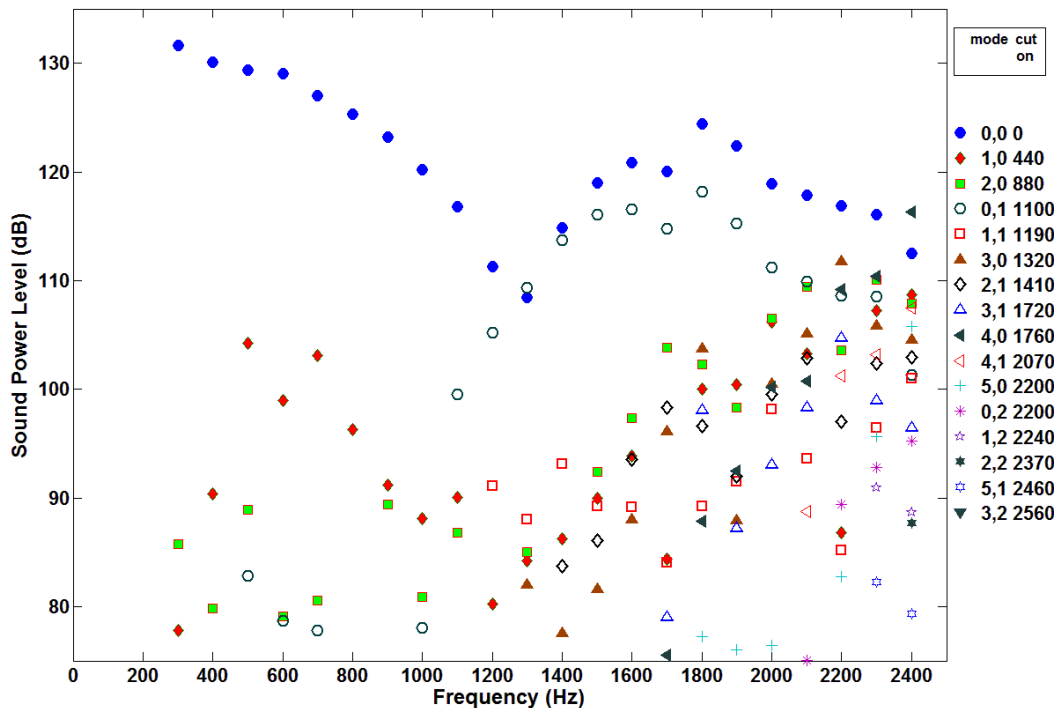


Figure 7. Mode distribution downstream of liner test section. (0,0) mode generated in the duct, flow speed Mach 0.275. Data acquired in 2010.

Figures 8 and 9 show the mode energy distribution downstream of the liner L01R at Mach 0.275 for the (1,0) and (2,0) mode, respectively, incident. In the same way that energy scatters from the (0,0) mode up to the (0,1) mode, Figure 7; energy is seen to scatter from the (1,0) to the (1,1), Figure 8; and from the (2,0) to the (2,1), Figure 9. This scatter is relatively weak and the incident mode still dominates downstream of the liner at most frequencies. The attenuation of the (2,0) mode, Figure 9, is not affected by the (2,1) mode at the peak as are the (0,0) and (1,0) modes.

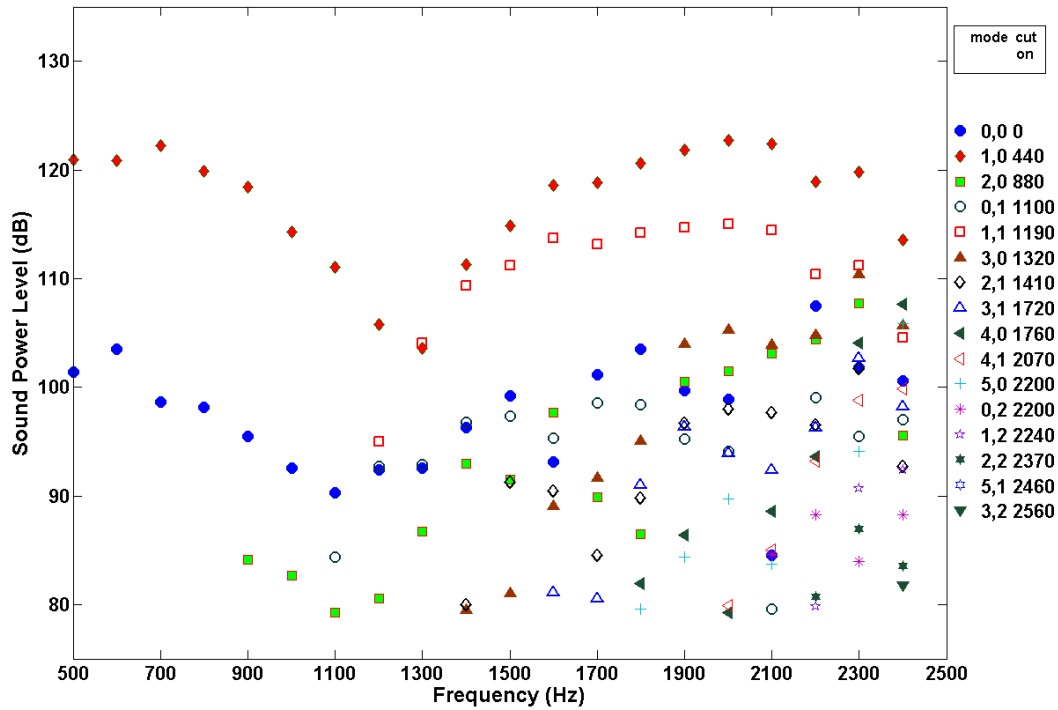


Figure 8. Mode energy distribution downstream of liner L01R, Mach 0.275, (1,0) mode incident.

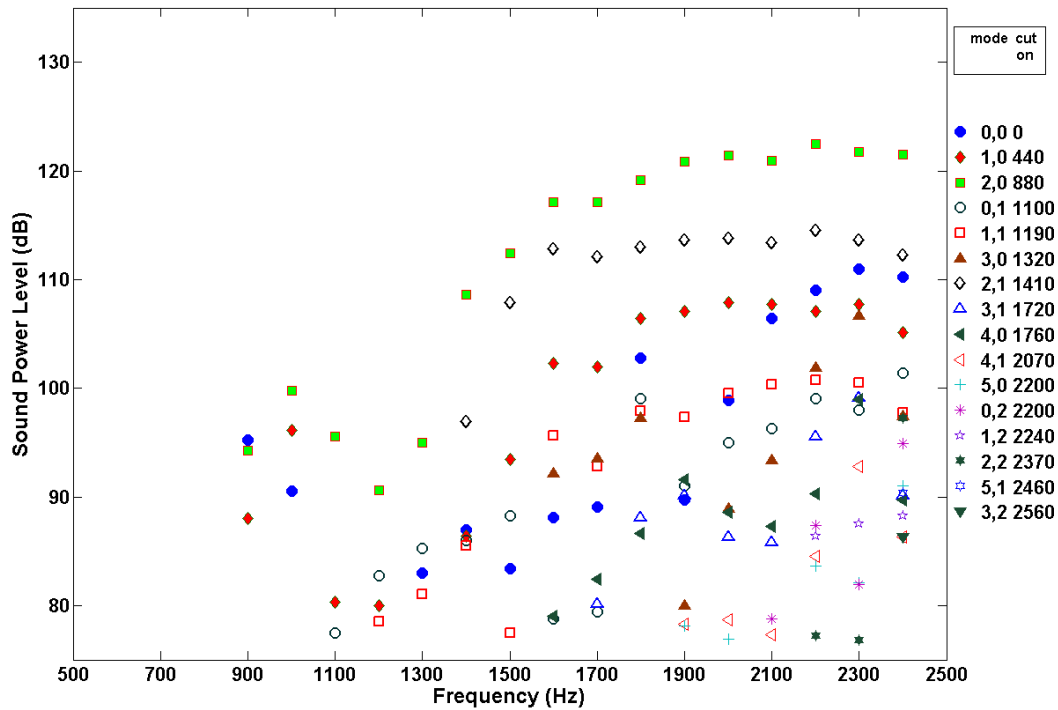


Figure 9. Mode energy distribution downstream of liner L01R, Mach 0.275, (2,0) mode incident.

Figure 10 shows the mode distribution downstream of the liner when the (0,1) mode is input. The energy scatter into the (0,0) mode is significant. At all frequencies, the overall sound energy downstream of the liner, and thus the attenuation, is strongly affected or dominated by the (0,0) mode. It was noted in the discussion on Figure 6 that, even though the (0,1) cuts on closest to the resonance of the liner, it is not the most attenuated. The strong presence of the (0,0) mode energy in the spectrum explains how the attenuation of the (0,1) mode is less than expected.

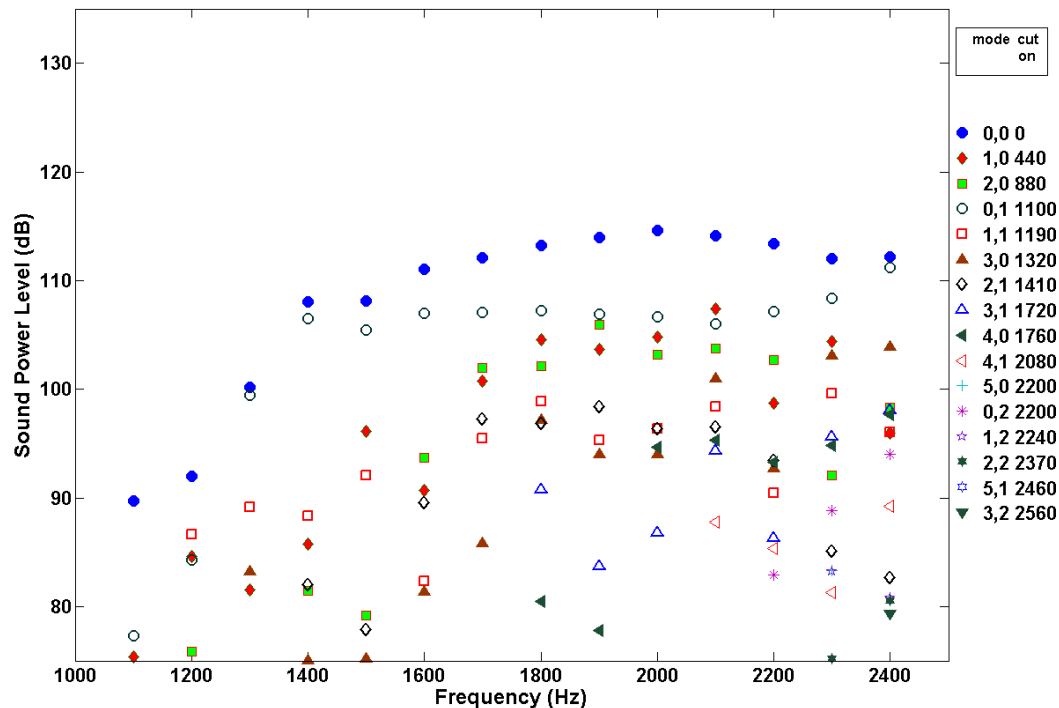


Figure 10. Mode distribution downstream of liner test section. (0,1) mode generated in the duct, flow speed Mach 0.275. Data acquired in 2010.

The modal energy distribution showed in Figure 8 that energy scatters from the incident (0,1) mode to the lower order (0,0) mode. A similar trend is shown in the energy redistribution from the incident (1,1) mode to the lower order (1,0) mode, Figure 11. Some energy scatters into the (2,0) mode, but generally the scatter is into the (1,0) mode. Figure 12 shows energy scatter from the incident (2,1) both to the (2,0) and to the (1,0) modes, but generally the scattered energy is dominant in the (2,0). The scatter into the next lower horizontal-order mode is quite strong and the mode into which energy is scattered generally dominates downstream of the liner.

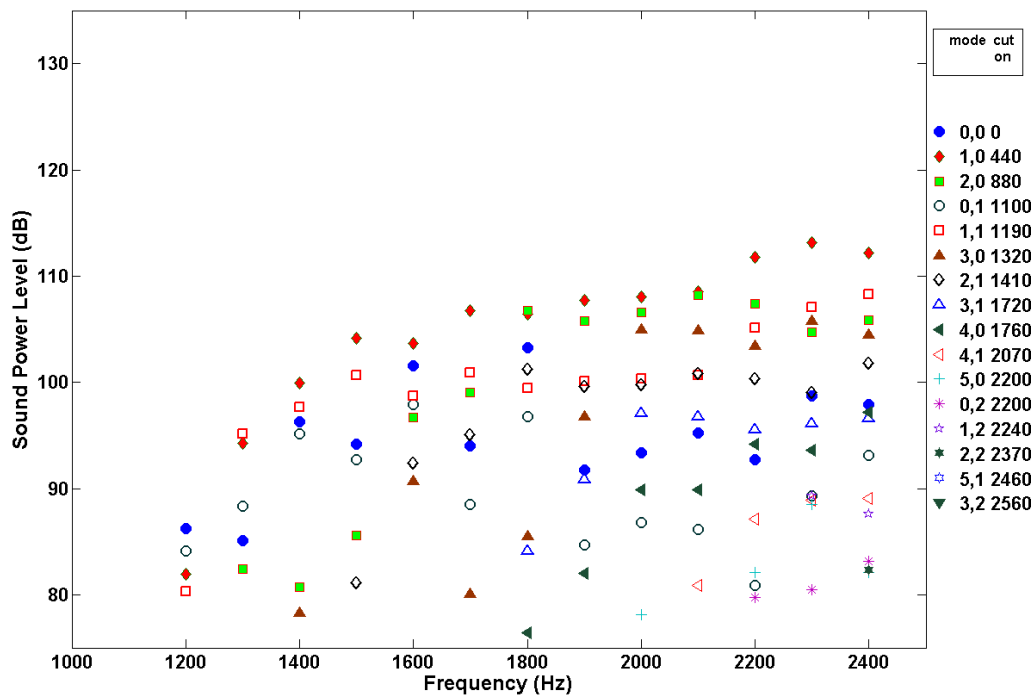


Figure 11. Mode energy distribution downstream of liner L01R, Mach 0.275, (1,1) mode incident.

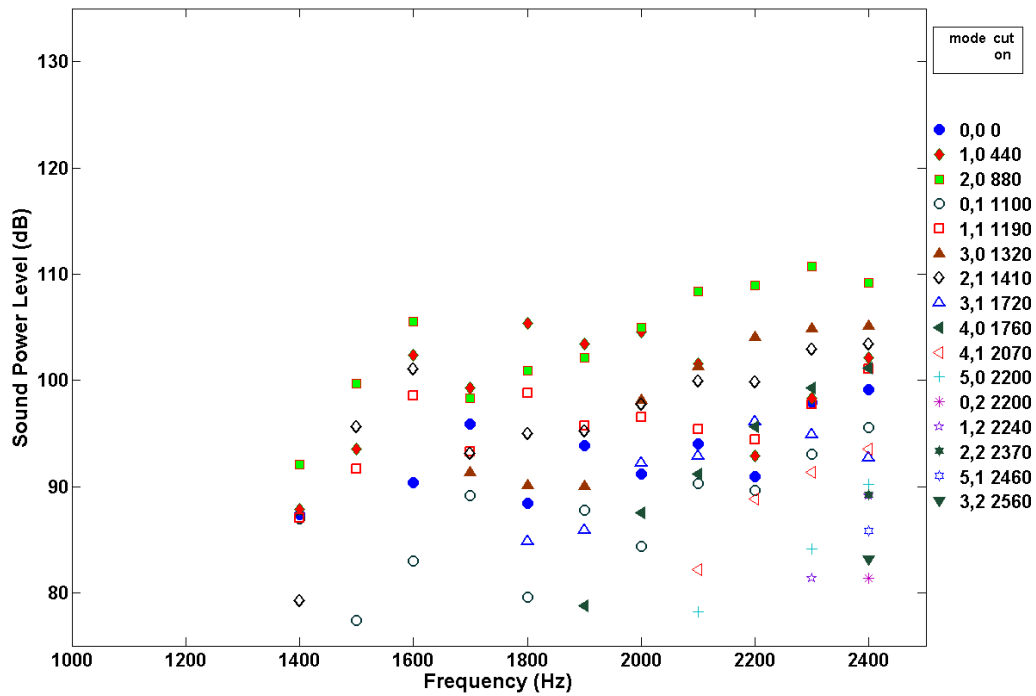


Figure 12. Mode energy distribution downstream of liner L01R, Mach 0.275, (2,1) mode incident.

The transfer of energy from the horizontal-order 1 mode to the lower order 0 mode is consistent with Kraft's discussion of energy shifting to a lower order, less attenuated mode [8]. His assertion that "the overall suppression is likely to be controlled by the second order mode, which is now least attenuated" is borne out by the results for the horizontal-order 1 modes.

There is no lower order mode into which the horizontal-order 0 modes can transfer energy, and the energy scatter from horizontal-order 0 to the more highly attenuated order 1 mode is not expected. The amount of energy transferred is not insignificant. Figure 13 shows the difference between upstream and downstream modal sound power for the case where the (0,0) mode is incident. The figure shows that most modes are, generally, attenuated or their power level is unchanged. The exceptions are the (1,0), (2,0), (0,1), (1,1), (3,0), (3,1), and (4,1) modes. Of these the most consistently amplified mode, particularly at frequencies above 1250 Hz, is (0,1), and the data indicate that this amplification could be as much as 15 dB. It was seen in Figure 7 that the (0,1) mode, while not dominant, contributes significantly to the downstream energy.

The strong energy transfer from horizontal-order 1 modes to horizontal-order 0 modes, and the less strong energy transfer from horizontal-order 0 modes to horizontal-order 1 modes is felt to arise from the lack of symmetry of the duct walls. The liner test section is acoustically soft on one wall and acoustically hard on the other. Once the incident axisymmetric mode is attenuated, the non-axisymmetric mode will be preferred in the non-axisymmetric duct. Likewise, the energy of the incident non-axisymmetric mode will scatter into the nearest symmetric mode. The energy transfer is strongest when the receiving mode is of lower order. The difference in mode scatter between a duct with one side acoustically treated and a duct with both sides treated was noted in a previous paper by the authors [5].

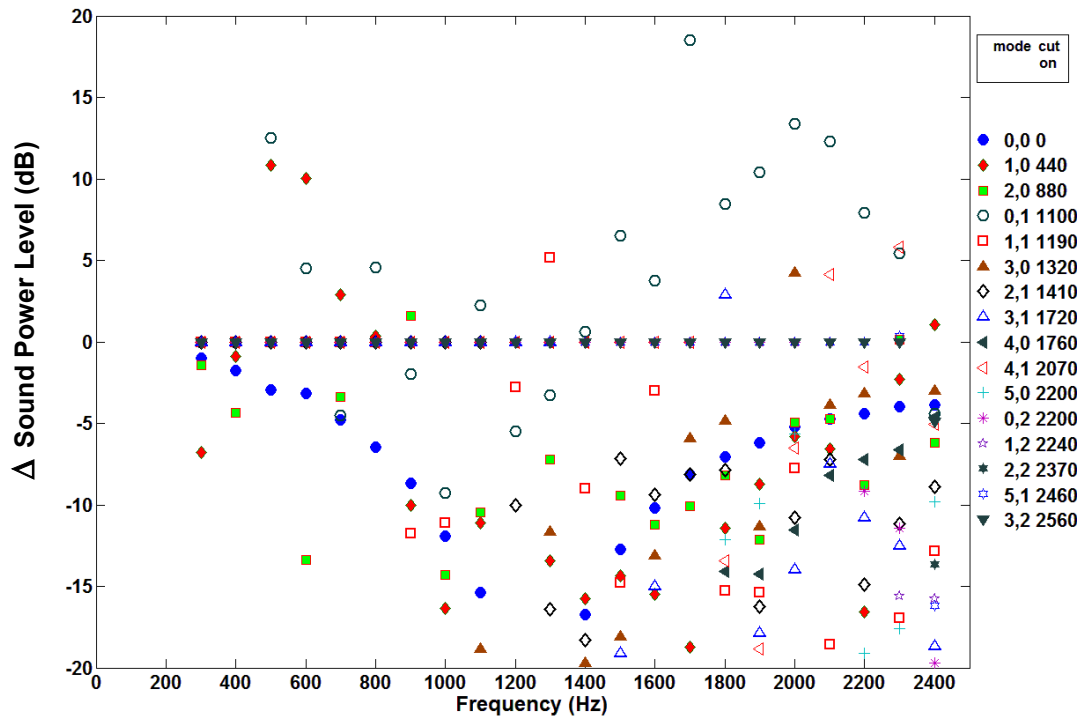


Figure 13. Change in mode power from upstream of the liner to downstream, configuration L01R (0,0) mode incident at Mach 0.275. Note, positive change indicates amplification of the mode power.

## 2. Data Processing: Results at Mach 0.500

It was shown in Figure 5 that the attenuation of the plane wave is significantly less at Mach 0.500 than it is at Mach 0.275. However, Figure 14 shows that the attenuation shifts to the higher order modes, and the peak attenuation of some of the modes at Mach 0.500 is on the same order as the attenuation of the lower order modes at Mach 0.275. As is seen in Figure 14, the peak attenuation occurs in the order 1 horizontal modes because these modes cut on near the frequency of peak attenuation, which has shifted up to the range of 1500 Hz. The attenuation increases from the (0,0) mode to the (1,0) mode as expected although it is not as great as at Mach 0.275 because the impedance of peak attenuation has shifted upward. Likewise, the attenuation of the (2,0) mode is greater than the (1,0) mode, and the dramatic increase of attenuation is unexpected.

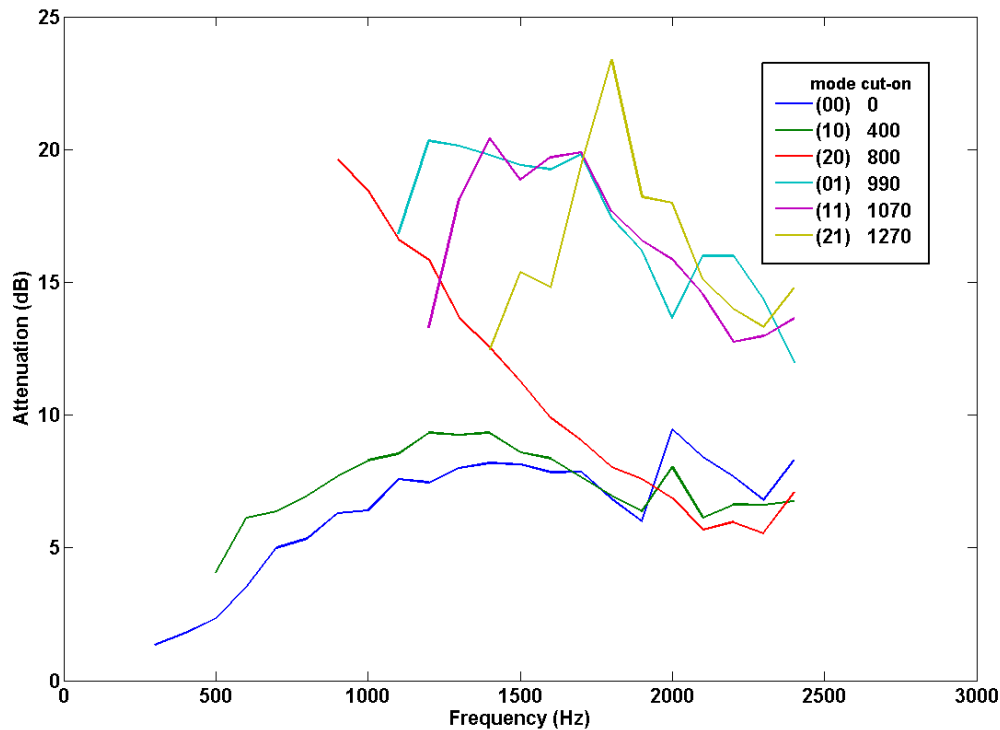


Figure 14. Attenuation of specified mode incident on liner test section with liner L01R at Mach 0.500

#### Mode distribution analysis:

The mode distributions downstream of the liner test section for various modes input to the duct at Mach 0.500 are shown in Figures 15-20. When the input mode is of 0 horizontal-order, that mode is dominant downstream, as is seen in Figure 15 for the (0,0), Figure 16 for the (1,0), and Figure 17 for the (2,0) mode. The mode of secondary importance in the distribution is the corresponding horizontal-order 1. This result is similar to the result at the lower flow speed, although at Mach 0.500 the energy in the order 1 mode is much less than the corresponding order 0 mode, where the order 1 mode was closer in magnitude to the dominant order 0 mode at Mach 0.275. The conclusion from the results at Mach 0.500 is the same as the conclusion from the results at Mach 0.275. Scattering of energy from the order 0 mode into the order 1 mode is felt to be due to the lack of symmetry of the acoustic treatment, hard on one side and acoustically soft on the opposite of the duct. The scattering effect is more pronounced at Mach 0.275 than it is at Mach 0.500.

When the horizontal-order 1 mode is input to the liner test section, energy is scattered into the corresponding order 0 mode and it is this mode which generally dominates downstream of the liner. Thus, the input (0,1) mode scatters energy into the (0,0) mode, Figure 18, the input (1,1) mode scatters energy into the (1,0) mode, Figure 19, and the input (2,1) mode scatters energy

into the (2,0) mode, Figure 20. The (0,0) mode clearly dominates in Figure 18. Dominance of the (1,0) mode in Figure 19 or the (2,0) mode in Figure 20 is less distinct. In fact, the (1,0) and (2,0) modes appear to have equal weight in the two plots. This is an unusual result. Mode shifting in the horizontal-order modes is expected because of the presence of the liner on the side walls. Since the upper and lower surface of the duct are hard walls, the vertical modes are expected to be orthogonal, and shifting energy into different vertical-order modes is not expected to occur. One possible explanation for this unexpected energy scatter is that the flow in the duct is not plug flow, as has been assumed in the mode decomposition routine, but has a finite boundary layer. The shear flow in the boundary layer could cause modes to scatter unpredictably, with the effect being greater at higher flow speeds.

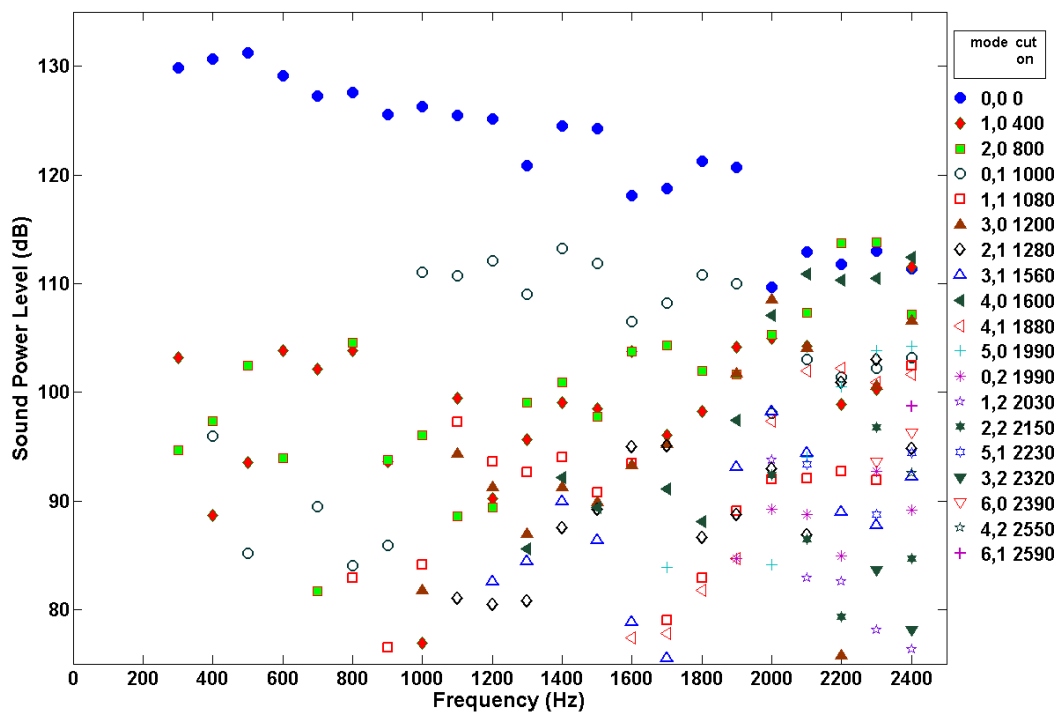


Figure 15. Mode energy distribution downstream of liner L01R, Mach 0.500, (0,0) mode incident.

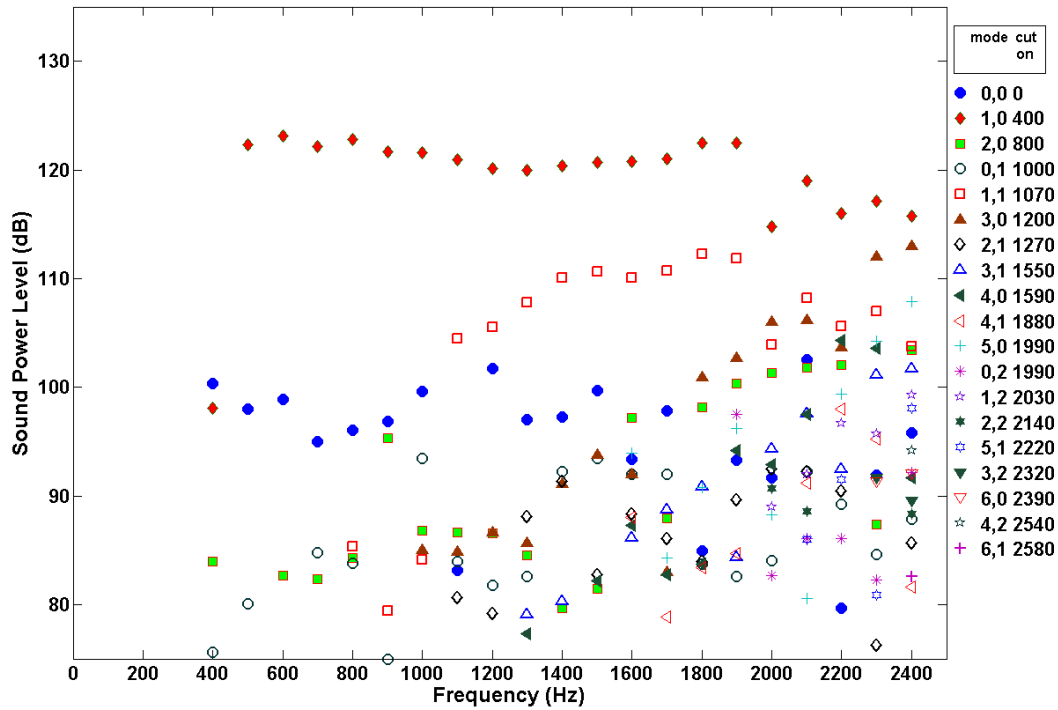


Figure 16. Mode energy distribution downstream of liner L01R, Mach 0.500, (1,0) mode incident.

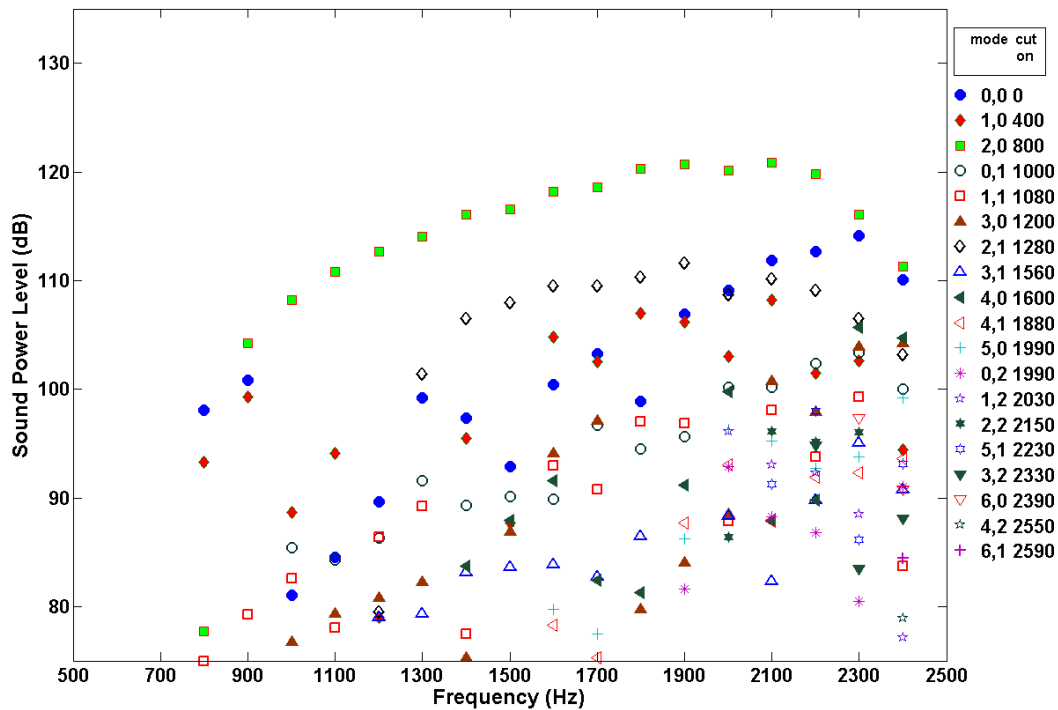


Figure 17. Mode energy distribution downstream of liner L01R, Mach 0.500, (2,0) mode incident.

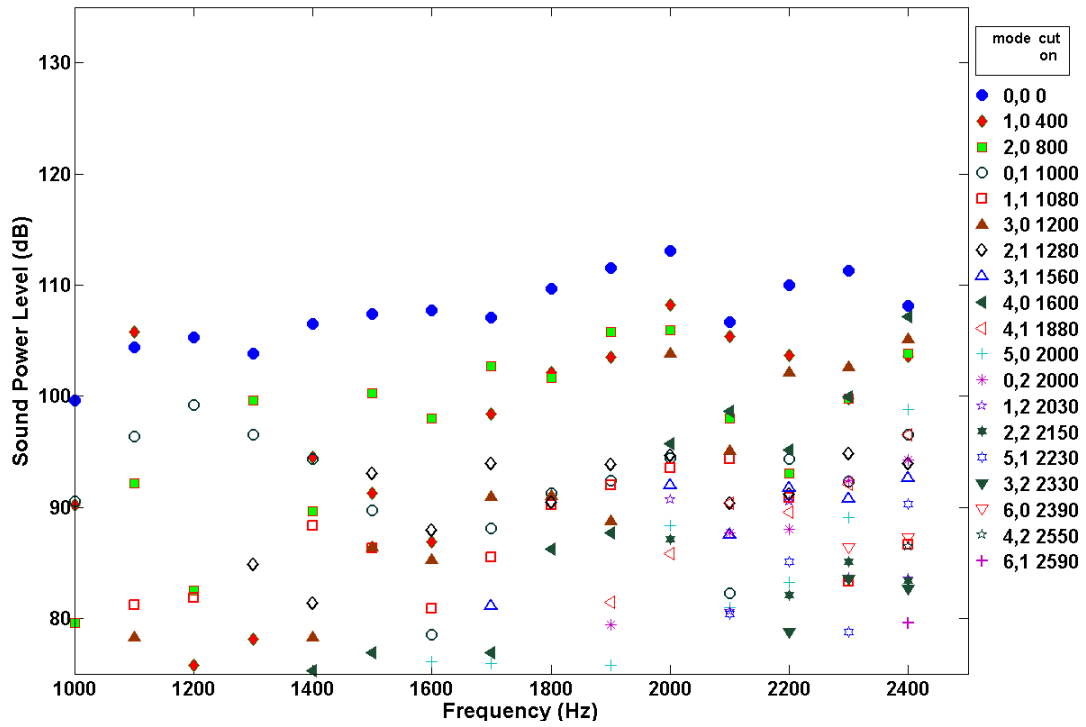


Figure 18. Mode energy distribution downstream of liner L01R, Mach 0.500, (0,1) mode incident.

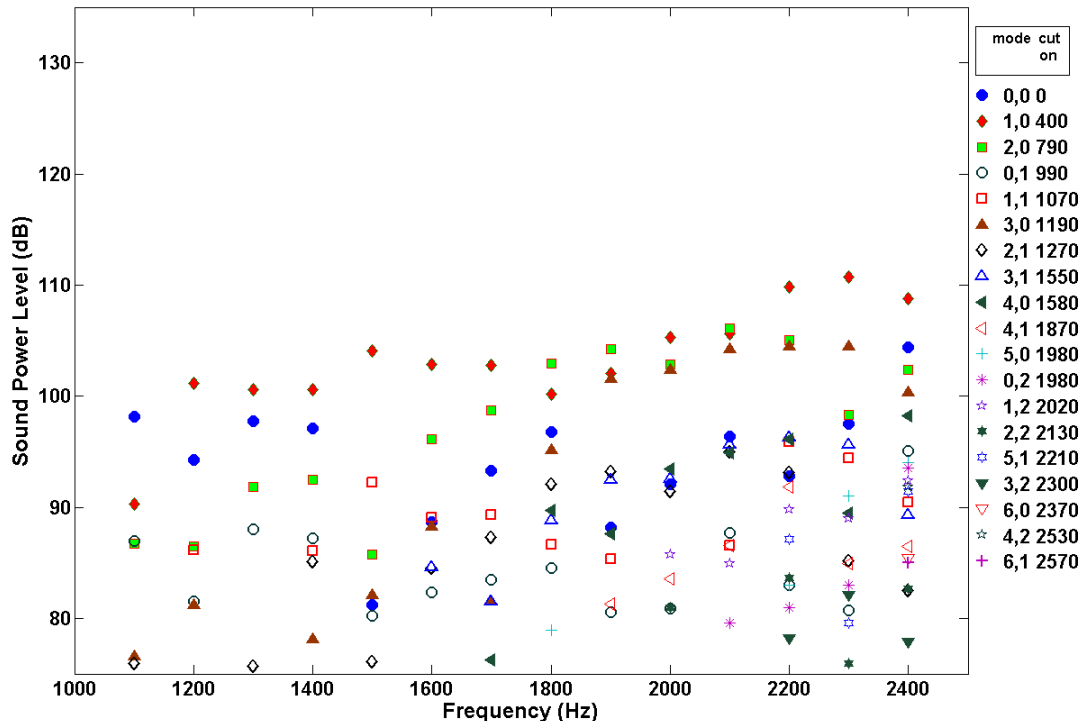


Figure 19. Mode energy distribution downstream of liner L01R, Mach 0.500, (1,1) mode incident.

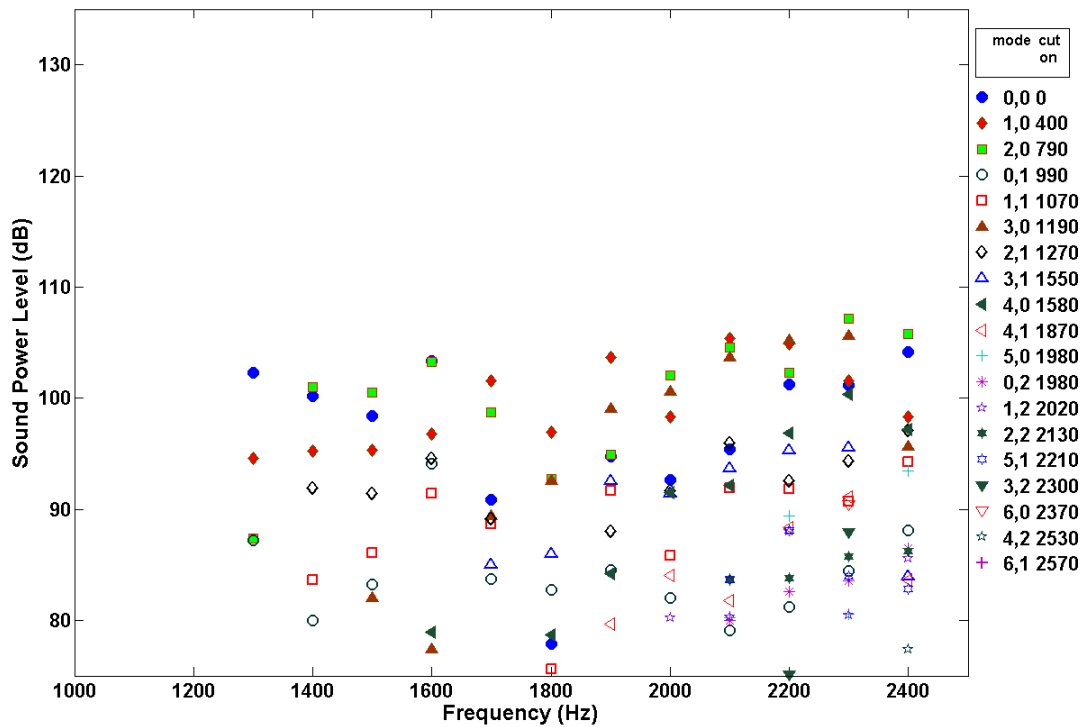


Figure 20. Mode energy distribution downstream of liner L01R, Mach 0.500, (2,1) mode incident.

#### IV. Summary

The move of the Curved Duct Test Rig has been successfully completed and the rig is fully operational. The research air supply has been changed from a high pressure source pushing air through the test section to a high capacity fan pulling air. This upgrade has resulted in significant increase in the flow speed capability in the test section. This allows testing and evaluation under more realistic flow conditions.

The baseline liner configuration, L01R, has been analyzed in the Curved Duct Test Rig. The tests showed that the upgraded research air supply produces results that are comparable to those obtained in the previous configuration at the same operating conditions. Enhancements have been made in the data analysis, which provide new insights into the acoustic performance of this liner configuration. The effect that flow speed has to shift the impedance spectrum is implied by the change of overall attenuation curves with flow speed. Further work is planned to quantify analytically and verify experimentally the change of impedance with mean flow in the duct. The effect that incident mode order has on overall attenuation in the duct has been shown. The general upward trend in attenuation at constant frequency with increasing mode order is

demonstrated. The scatter of energy from the incident mode into a lower-order, less-attenuated mode is shown. The resultant energy downstream of the liner is, in most cases, dominated by the lower-order mode. This is clearly shown at Mach 0.275. At Mach 0.500, the mode scatter is less predictable, and it is felt that the non-uniformity of the flow causes anomalies in the scattering.

Energy is also seen to shift from the horizontal-order 0 modes into the horizontal-order 1 modes, although this energy shift is relatively weak. This shift is felt to arise from the asymmetric design of the acoustic treatment in the duct. The capability to shift energy into higher or lower order modes has significant implications in terms of liner treatment designs for specific noise sources. Future research in this area will include analysis of other symmetric and non-symmetric liner configurations, and investigation of the mode scatter by higher horizontal-order modes. The enhanced experimental and data analysis capabilities in the Curved Duct Test Rig are expected to improve our understanding of the effect of liners on sound propagating in the duct and to help in development of higher fidelity duct acoustic treatments.

### **Acknowledgements**

The authors are grateful for contributions made to the successful completion of this project by the laboratory technician staff and in particular Christal Kellam of NASA LaRC for experiment set-up and data collection. NASA's Subsonic Fixed Wing Project of the Fundamental Aeronautics Program funded this work.

### **References**

1. Groeneweg, J.F., Sofrin, T.G., Rice, E.J., and Gliebe, P.R., Chapt 3, "Aeroacoustics Of Flight Vehicles: Theory And Practice, vol 1: Noise Sources", NASA RP 1258, vol 1, August 1991.
2. Gerhold, C., Brown, M., Jones, M., and Nark, D., "Investigation of liner characteristics in the NASA Langley Curved Duct Test Rig," AIAA Paper 2007-3532, May, 2007.
3. Gerhold, C., Cabell, R, and Brown, M., "Development of an experimental rig for investigation of higher order modes in ducts", AIAA Paper-2006-2637, May 2006.
4. Jones, M.G., Parrott, T.L., and Watson, W.R., "Comparison of Acoustic Impedance Eduction Techniques for Locally-Reacting Liners," AIAA Paper 2003-3306, Proceedings of the 9th AIAA/CEAS Aeroacoustics Conference & Exhibit, May, 2003.
5. Gerhold, C.H., Brown, M.C., Jones, M.G., Nark, D., and Howerton, B.M., "Configuration effects on the acoustic performance of a duct liner", AIAA paper 2008-2977, May, 2008.
6. Motsinger, R.E and Kraft, R.E, "Design and performance of duct acoustic treatment", Chapt 14, "Aeroacoustics of flight vehicles: theory and practice, vol 2: Noise Control", NASA RP 1258, vol 2, August 1991.

7. Rice, EJ and Heidman, MF, "Modal propagation angles in a cylindrical duct with flow and their relation to sound radiation", AIAA paper 79-0183, 1979
8. Kraft, R.E., "Theory and measurement of acoustic wave propagation in multi-segmented rectangular flow ducts", report number R77AEG585, General Electric Technical Information Series, Oct. 1977